SAND2000-2378J

L-shell emission from high-Z solid targets by selective inner-shell collisional electron ejection

T.R. Nelson[1,2], A. B. Borisov[1], K. Boyer[1], S. Cameron[2], J. W. Longworth[3], T.S. Luk[2], A. McPherson[4], W. A. Schroeder[1], J. Santoro[1], A.J. Van Tassle[1] and C. K. Rhodes[1].

1. *Department of Physics (M/C 273), University of Illinois at Chicago, 845 W. Taylor Street, Chicago, IL 60607-7059, USA*
2. *Sandia National Laboratories, Albuquerque, NM 87185*
3. *Illinois Institute of Technology, Chicago, IL 60616-3793*
4. *Argonne National Laboratory, Argonne IL, 60439-4800*

Abstract

Evidence of highly efficient (1.2% yield) x-ray emission from Ba(L) (2.4 – 2.8Å) and Gd(L) (1.7 – 2.1Å) produced from extensively ionized atoms in laser-excited plasmas in BaF_2 and Gd solid targets is presented. An analysis describing a *shell-selective, coherent* collisional ionization mechanism is also given in order to explain the observed highly efficient hollow atom production in solids. The L-shell spectra were observed as a result of intense irradiation (peak intensities of 10^{18}–10^{19}W/cm^2) generated by a sub-picosecond ultraviolet (248nm) terawatt (1TW = 10^{12}W) laser system driven by a hybrid Ti:Sapphire/KrF* laser system. A mica-crystal von Hámos spectrograph equipped with Kodak RAR 2492 x-ray film and appropriate filters was used to collect the spectra emitted by the targets. We also discuss the limitations on producing this type of radiation imposed by the laser system used in the experiments and propose a method for surpassing this limitation with little or no additional effort or expense in order to produce L-shell radiation on the order of 15–17 keV from targets as heavy as Uranium.

DISCLAIMER

I. Introduction

Recent studies have reported the extremely efficient production of multi-kilovolt x-ray radiation resulting from inner-shell transitions in rare gas clusters [1-6] as a result of intense irradiation with a subpicosecond ultraviolet (248nm) laser. In particular, the spectra of these emissions were highly anomalous; $2p$ vacancies were being readily produced while the outer subshells remained largely *unperturbed*. This property seems extremely promising for achieving population inversion in these rare gas clusters and leads to the *coherent amplified emission* of these highly energetic x-rays.

In an attempt to explain the properties of this anomalous x-ray generation, Schroeder et. al. [7,8] proposed a new collisional ionization process in which the ponderomotively-driven electrons retained a substantial portion of their phase and symmetry (i.e. coherence) from their original atomic state for a brief period of time after ionization. In reference [8], the authors found it necessary to consider the quantum mechanical wavefunctions of the ionized electrons when examining the ionization cross sections for the ejected $2p$ electrons. This is due to the fact that although it has been shown that a conventional collisional ionization process may produce large ionization rates in rare gas clusters for sufficiently high intensities [20], this approach fails to explain both the anomalous nature of the observed spectrum as well as the observed wavelength scaling of the production of the Xe(L) radiation from clusters [6]. In fact, a calculation of the plane wave collisional cross sections for the specific electron orbitals yields a cross section for the ionization of a $3s$ electron that is an order of magnitude *greater* than that for the $2p$ electrons [7,21]. This does not agree with the observations published in [1,6], which show large radiative yields from electronic states with $2p$ vacancies where the $3s$ subshell is largely intact.

However in reference [7], as a result of the distinctive quantum mechanical treatment of the laser-driven electrons, the collisional ionization dynamics were significantly altered in such a way as to yield a significant n-state and l-state selectivity. In the case of Xe(L) radiation, the assertion was made that it was the previously ionized $4p$ electrons which were acting to generate the $2p$ vacancies. Given that the net result of this process was the deposition of ~8keV (the ionization potential of Xe $2p$ electrons) of energy into the target ion over the course of one laser cycle (0.8fs), the result is a power coupling in excess of 1W/atom. However, the theory outlined in references [7,8] is based upon the supposition that the pondermotively driven photoionized

electron subshell is able to propagate unperturbed by external interactions until it returns to the cluster or ion of origin. In the case of a solid material, this assumption is not valid due to the increased density of atoms in the vicinity of the parent ion.

In this paper, hollow atom L-shell spectra will be presented from two solid targets, Ba(L) and Gd(L). The spectra provide evidence of this shell-selective collisional ionization mechanism in solid density targets, and the application of the theory to high-density targets will be discussed. In addition, two Gd(L) spectra observed under different laser intensities will serve as the basis to establish an upper bound on the hollow atom x-ray generation based on the peak laser irradiance, and a method of extending this limit with the current laser source will be examined.

II. Experimental Setup

The laser system used for the generation of the spectra presented in this paper is a Ti:Sapphire/KrF* hybrid system which is similar to that outlined in reference [9], with the exception that the infrared amplification stage has been replaced by a Ti:Sapphire regenerative amplifier [10]. The system produces pulses with an average energy of 400mJ and pulse duration of 230fs. An f/2 parabolic optic was used to focus the 248nm laser pulse into the target for a resultant focal intensity of $\sim 10^{19} W/cm^2$. The spectra were recorded using a mica-crystal von Hámos spectrograph in 3rd order and Kodak RAR 2492 film. A 100μm Kapton (polyimide) filter was used in front of the spectrometer to block lower energy (M-shell) photons. The targets used were a BaF_2 optical flat to generate the Ba(L), and a 100μm thick Gd foil, mounted on an Al substrate.

III. Experimental Data

Figure 1 shows the recorded Ba(L) spectrum. The spectrum was produced under intense irradiation by a pulse energy of 320mJ, corresponding to a laser power of 1.4TW and a focal irradiance of $\sim 10^{19} W/cm^2$. As can be seen from the figure, the double-peaked structure characteristic to the 3d→2p transition [11] is present, with charge states ranging up to 38+ at the peak of the spectrum, as labeled in Figure 1. By comparison with the Xe(L) spectrum described in reference [1], transitions ranging from ($2p^6 3d^9 \leftarrow 2p^5 3d^{10}$) to ($2p^6 \leftarrow 2p^5 3d$) are present in the

spectrum. In addition, the Ba spectrum displays the prominent characteristic solid state transitions L_α, $L_{\beta 1}$ and $L_{\beta 2}$ from weakly ionized (0 – 10+) Ba atoms.

To illustrate the efficiency of the x-ray yield, a calibrated diamond photoconductive semiconductor device (PCD) was used for the BaF_2 target. A trace from this detector is shown in Figure 2. The temporal width of the signal is limited by the response of the detector. A filter of 0.1 um thick Al on a 7.6 um thick Kapton substrate was used to block radiation from Ba(M). The signal shown in Figure 2 corresponds to a total energy of ~4.9mJ, assuming a uniform 2π distribution. This translates into a conversion efficiency of ~1.2%! In addition, the risetime of the detector signal is on the order of 100ps, with a <200ps decay, which is limited by the response of the detector and oscilloscope (Tektronix SCD5000). This is in stark contradiction with the observations of Ditmire, et al., which showed a long lived emission on the order of ~1ns [5,20] from Kr clusters, and supports the conclusion that the Xe(L) emission is prompt and could be as short as the lifetime of the laser pulse. However further experiments with greater temporal resolution (i.e. fast x-ray streak camera measurements) are required to prove this assertion.

Shown in Figure 3(a) and 3(b) are two Gd(L) spectra taken under identical experimental conditions, with the exception of the peak laser intensity. As in the Ba(L) spectrum, Figure 3(a) shows the usual hollow atom spectrum with charge states ranging up to 40+, in addition to the solid state lines $L\alpha_1$ and $L\beta_1$ from weakly ionized Gd atoms. The incident laser pulse energy was 350mJ, corresponding to a laser power of 1.5TW (irradiance of ~10^{19}W/cm^2). In Figure 3(b), the hollow atom spectrum is absent, leaving only the solid state lines. The laser pulse energy in this case was 200mJ, a factor of 0.6 lower. As will be discussed in the next section, the information yielded by the two spectra provides crucial evidence to support the theory presented in this paper and in reference [8].

IV. Solid Target Shell-Selective Collisional Ionization Theory

As indicated in section I, the theory outlined in the reference [8] makes the assumption that the pondermotively driven 4p electron subshell is unperturbed by external collisions until it returns and collides with the parent ion or cluster. The cross-section for this interaction is proportional to the modulus square of the matrix element M_{fi} associated with the interaction mechanism which, for an initial state $|i\rangle$ coupled to a final state $|f\rangle$ through the interaction potential V, is written as

$$M_{fi} = \langle f|V|i\rangle \,. \tag{1}$$

It was shown in reference[8] that M_{fi} may be expressed as

$$M_{fi}(\mathbf{R}=0) = \iint d^3\mathbf{r}_1 d^3\mathbf{r}_2 \frac{\phi_j(\mathbf{r}_1)\psi(\mathbf{r}_2,t)}{r_1 r_2|\mathbf{r}_1-\mathbf{r}_2|}\exp[-i\mathbf{k}_1.(\mathbf{r}_1-\mathbf{r}_2)]\,, \tag{2}$$

where $\phi_j(\mathbf{r}_1)$ is the wavefunction of the electrons to be collisionally ionized, located at coordinate $\mathbf{r}_1$ around the atom, $\psi(\mathbf{r}_2,t)$ is the wavefunction of the ponderomotively driven electrons, located at coordinate $\mathbf{r}_2$ about the center of the photoionized electron cloud, $\mathbf{k}_1$ is the wave vector of the ejected electron after the collision, and $\mathbf{R}$ is the displacement vector between the atom and the electron cloud.

In reference [8], the value of M_{fi} was evaluated and compared for UV (248nm) and IR (800nm) wavelengths, based on the assumption that the collisional ionization occurred after one laser period. This assumption was reasonable because of two points. First, it was demonstrated in reference [7] that it was kinematically possible, for sufficiently high laser intensities, that a previously ionized electron may collide with the cluster of origin with more than enough kinetic energy to ionize a $2p$ electron from Xenon (~8keV). Second, it was estimated that the intracluster separation in the target gas jet was large enough such that the electrons could be accelerated back into the parent cluster unperturbed by collisions with other clusters.

However, in a solid density material, the assertion of a collisional ionization occurring in the parent atom is not generally valid. Since the theory governing the ionization of the electron wave packet is unaffected by the target density, it is still reasonable to assert that the 4p electrons retain their previous quantum mechanical radial and angular distribution for some period of time after ionization. The primary difference introduced by the target density is that in this case, the dephasing time could be much shorter, due to the fact that it is possible for the electron wave packet to be dephased by electron-ion collisions in addition to internal electron-electron scattering. However, the crucial point to be made here is that in general, there is *no reason* why the 2p vacancies must be created in the *same ion from which the 4p electrons originated.* That is, *this enhanced coupling is not dependent on the specific ion of origin,* only the quantum

mechanical nature of the electron wave-packet. Differences between ions such as actual ionization state will have a small effect on the specific bound 2p wave functions, however, this will only change the magnitude of $|M_{fi}|^2$ by a modest amount; the physics governing the interaction remains unchanged. In fact, compared to the gas cluster case the coupling should be *greater* in solid targets due to the fact that the electron orbital will have had less time to dephase due to internal electron-electron collisions. Also the overlap should be greater because the intrinsic spreading of the wave packet will not be as progressed.

At this point, to evaluate whether this shell-selective collisional ejection theory may be applied to solid targets, the only issue remaining to be considered is whether the pondermotively driven electrons will have enough kinetic energy to eject a 2p electron from the target ion. In order to answer this question, two pieces of information are required: (i.) the kinematics of the pondermotively driven electrons (i.e. the kinetic energy as a function of position or time) and (ii.) the approximate distance between ions. The first point listed above has been calculated in reference [7]. Specifically, the authors used a classical relativistic model to trace out both the position and kinetic energy of the ponderomotively driven electrons as a function of time (Figure 4). The calculations in Reference [7] were performed for Xe clusters, however, the numbers are sufficiently similar to those of Ba to be applicable; the ionization potentials differ only by ~5% and the Xe, cluster radius r_c for the calculations was 5.3Å, while the lattice spacing in BaF_2 is ~6Å. Therefore, for simplicity, all calculations performed here will be done for Ba, although qualitatively there will be little difference in the results for Gd.

To address the second point, one finds that estimating the distance between ions may be extremely complicated. In order to quantify this parameter, detailed knowledge of the plasma density generated by the laser is required. In general, this measurement may be very difficult [12]. In addition, due to the high density of ions near the ion of origin for the electrons, a rigorous Monte-Carlo simulation must be done to approximate the average frequency of collisions. While these details are necessary in order to precisely estimate the magnitude of $|M_{fi}|^2$ for each solid target, they are not required to ascertain whether the theory may be applied. These calculations are beyond the scope of this paper, and are instead left for future work on this subject.

In order to determine whether the theory may be applied at all may then be answered simply by establishing realistic upper and lower limits for the ion separation in the laser-driven

plasma. Clearly, a reasonable upper limit for the interaction distance is that of the gaseous target. It has already been shown in reference [8] that the theory readily applies to this case. For a lower limit, a first approximation would be the actual lattice spacing of the unperturbed solid. A typical number for this spacing is in the range of 5Å. As can be seen from Figures 4(a) and (b) [7], after traveling this distance, an electron will *not* have the required kinetic energy to ionize a 2*p* electron. However, it can be easily argued that this lower limit of the unperturbed lattice spacing is unrealistically small. In Reference [13], Ditmire et al. showed that medium sized clusters (~30Å) can increase their radius by as much as an order of magnitude under intense (10^{16}W/cm^2) irradiation within the first half of the laser pulse (~70fs), due mainly to hydrodynamic and coulomb forces within the cluster. While a solid target will be more constrained by the higher density of the surrounding material, the laser intensity for these experiments is 3 orders of magnitude in excess of that used for the above study. Furthermore, from examining Figure 4, it is seen that the average atom separation need only increase by a *factor of two* to allow the electrons sufficient time to accelerate to energies large enough to ionize a 2p electron. Therefore, using an ionic spacing on the order of 10-20Å as an extremely conservative lower bound is not only reasonable, but sufficient to demonstrate that the theory may be applied to the case of solid targets.

In addition, the argument may be made that although there are a high density of atoms near the parent ion, the probability of the ponderomotively driven electrons interacting with an ion is less than unity. Therefore it is entirely possible that the electrons do not interact with the nearest neighbor ion, thus allowing them to be further accelerated to gain sufficient energy to eject the 2p electrons from next-nearest neighbor ions.

At this point a qualitative estimate of the effects on $|M_{fi}|^2$ for a given solid may be made. Figure 5(a) and (b) show a plot of $|M_{fi}|^2$ for Barium. As in reference [8], the matrix element is a function of the parameter κ, which is defined as $\kappa = -k_1\cos\beta$, with β equal to the angle between $\mathbf{k}_1$ and the vector $\mathbf{r}_1 - \mathbf{r}_2$. Lower values of κ were used in generating the curve, ($\kappa = 9.9$Å^{-1} for the 2p case, and 16.2Å^{-1} for the 3p case) than in the Xenon case [8] to reflect the fact that in general, the electrons may have lower energy when incident on the target ion due to the reduced time from photoionization to the first collision. Qualitatively, it may be seen that as t/τ decreases for the time of collision, the value of $|M_{fi}|^2$ will increase for the ultraviolet driving laser case. Also, for very small ion separations, the actual time t before collision for the infrared case will move

closer to that for the ultraviolet case. In the limiting case of the lowest possible time before collision, the wavelength dependence would be severely reduced, since the collision time would become primarily a function of the ion spacing, and not the laser period. However, at this time there are no data for the infrared case in these solid targets to either confirm or disprove this assertion.

V. Limitations on X-Ray Generation

As was mentioned previously in section III.B, the L-shell spectra for Gadolinium serve to establish an upper bound for the ability to generate L-shell hollow atom spectra for this laser system. In addition, using the theory discussed herein allows the data to provide a quantitative means of predicting this ability as a function of laser intensity.

Figure 3 (a) and (b) show two Gd(L) spectra taken at laser intensities which differ by roughly a factor of 1.6. In case (a), the laser intensity is sufficient to produce the hollow atom spectrum, while in case (b), it is conspicuously absent. As is shown in Table I, a peak laser intensity of approximately 1.4 x 10^{19}W/cm^2 is required to ionize the entire 4p subshell by ATI theory [14–16], as is given by equation (3),

$$I_{ATI}\left(W/cm^2\right)=\frac{4\times10^9\left(I_p(eV)\right)^4}{Z^2} \tag{3}$$

where I_p is the ionization potential of the electronic state to be ionized, and Z is the charge of the residual ion. This implies that the peak laser intensity must be on the order of ~2 x 10^{19}W/cm^2.

An independent estimate of the laser focal intensity can be made from the laser parameters of a power of 1.5TW and a measured ~3μm focal diameter (diffraction limited diameter is 2.4μm for a flattop beam profile). These numbers yield an approximate peak focal intensity of ~4 x 10^{19}W/cm^2, which is in agreement with the above result.

At this point, a map may be constructed showing the laser intensities required to produce this hollow-atom L-shell spectrum as a function of Z for a range of elements. This map is shown in Figure 6. The elements are plotted according to the laser intensity required to ionize the respective 4p subshells for the various elements as a function of Z for a range of elements spanning the periodic table. Indicated on the map is the current limitation of the laser system

described in section II, which occurs just past Gd, allowing for the production of x-ray photon energies of ~6keV.

Although this range can be extended by increasing the laser intensity by conventional means, it is more advantageous to take make use of a current well-known physical effect to increase the laser intensity by orders of magnitude at *virtually no additional expense or effort.* By focusing the laser into an underdense plasma, the beam can be made to self-focus, creating a channel in which the peak intensity is in excess of 10^{21}W/cm^2 [17]. These channels have been readily observed in gas cluster targets [17,18]. Moreover, recently the authors of reference [19] used a pre-pulse consisting of ~15% of the total laser energy to create an underdense plasma in front of a solid target, allowing the main laser pulse to channel in the plasma. As a result of the increased laser intensity, the authors reported observing up to 2.5MeV γ photons produced by Bremsstrahlung as a result of the increased kinetic energy of the ponderomotively driven electrons. Alternatively, the solid target could be positioned behind a suitable gas cluster target (Kr or Xe) in order to form a channel before the solid target. A third option would be to use a metal with a suitably low boiling point such as Bi, to form clusters of the high Z solid, in order to facilitate channel formation in the material. Utilization of any of these techniques could readily increase the laser intensity by 2 orders of magnitude, thus allowing for the generation of hollow atom L-shell spectra as energetic as 15keV from a Uranium target, as is shown in Figure 6.

VI. Conclusion

In this paper, we have demonstrated the generation of L-shell radiation with energies in excess of 5keV from Ba and Gd targets with efficiencies on the order of 1%. The mechanism attributed to this high efficiency is an inner-shell selective collisional ejection process in which the laser energy is coupled into the target at a rate in excess of 1W/atom. The two Gd(L) spectra shown provide direct support for this theory of collisional ejection when correlated with the ionization potentials for the Gd 4*p* electrons. Finally, this paper provides a means of predicting the ability to produce L-shell spectra from highly ionized plasmas as a function of laser intensity, and describes a simple method for producing hard x-rays from elements spanning the periodic table up to and beyond 15keV U(L) radiation.

VII. Acknowledgements

Support for this research was partially provided under contracts with the Army Research Office (DAAG55-97-1-0310), and Sandia National Laboratories and the United States Department of Energy (DE-AC04-94AL85000 and BB9131). Sandia is a multi-program laboratory operated by Sandia Corporation, a Lockheed Martin company, for the United States Department of Energy under contract DE-AC04-94AL85000. A. McPherson is supported by the United States Department of Energy, Office of Science, under contract #W-31-109-ENG-38.

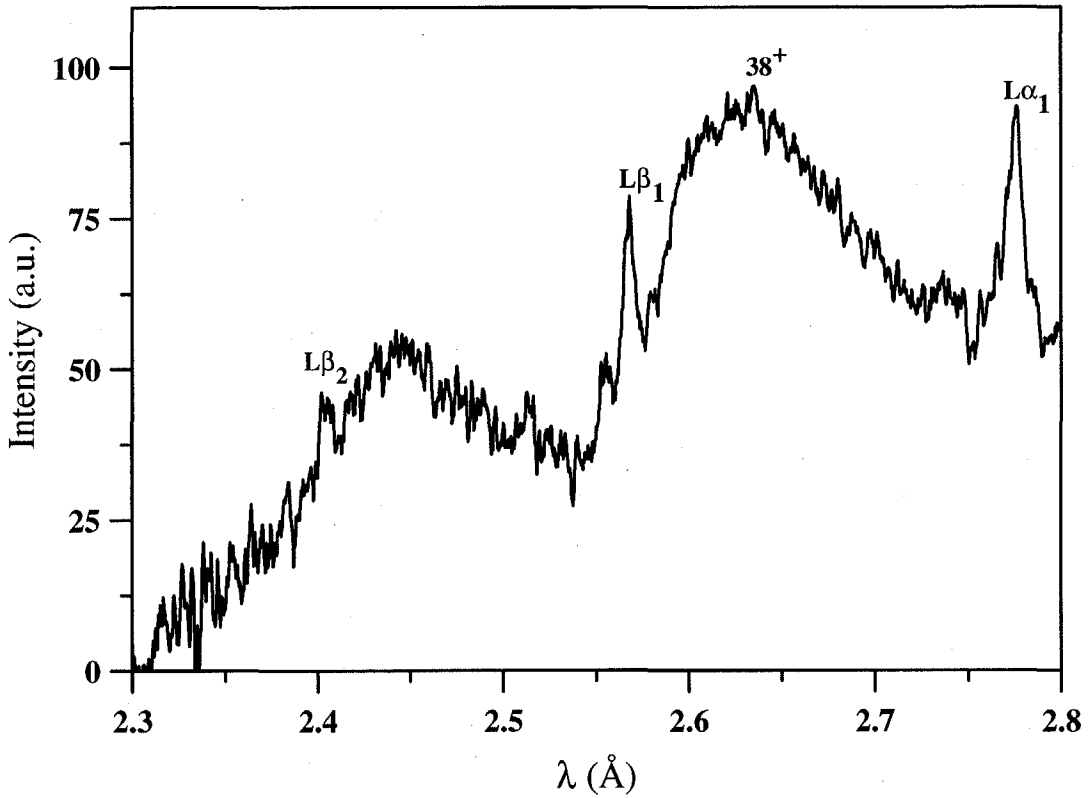

Figure 1

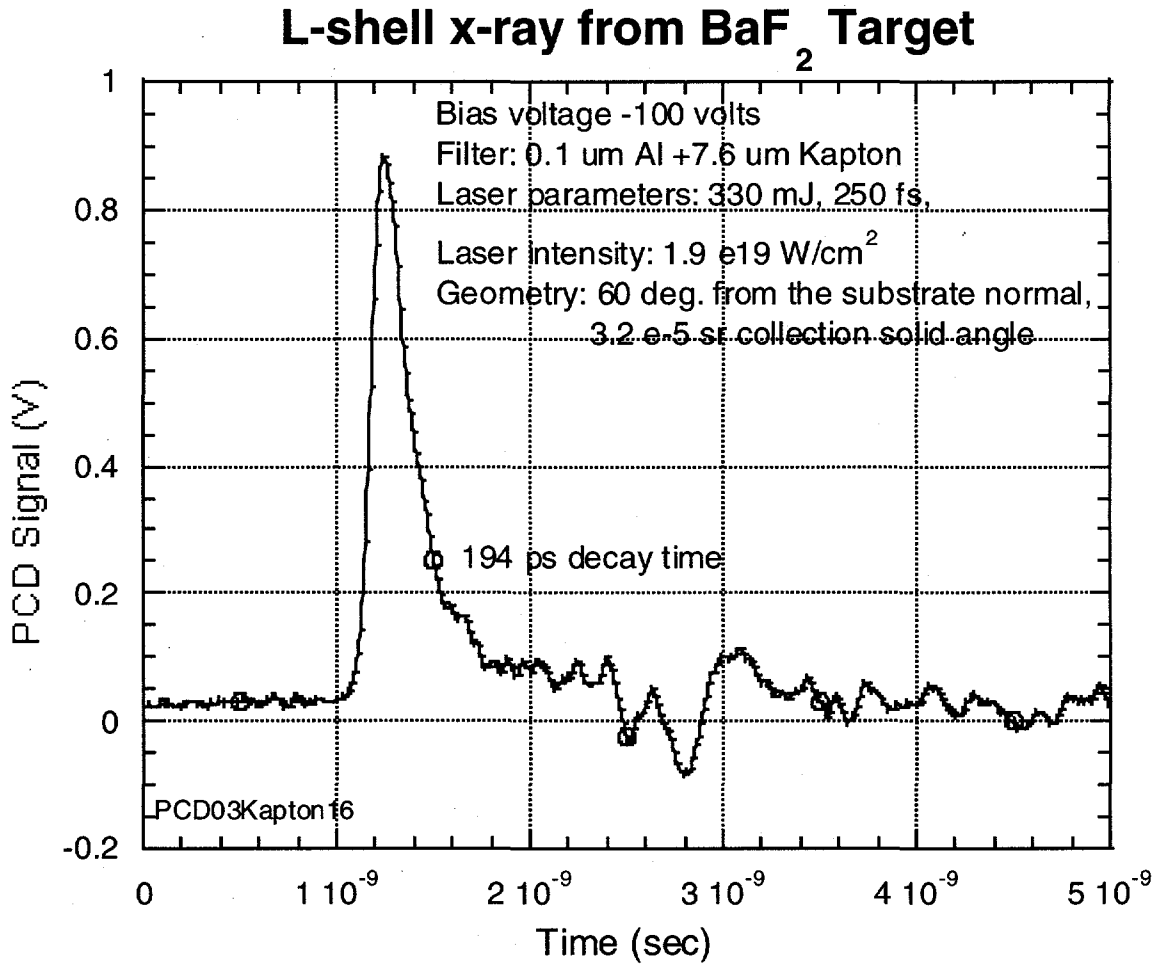
L-shell x-ray from BaF2 Target
Bias voltage -100 volts
Filter: 0.1 um Al +7.6 um Kapton
Laser parameters: 330 mJ, 250 fs,
Laser intensity: 1.9 e19 W/cm2
Geometry: 60 deg. from the substrate normal,
3.2 e-5 sr collection solid angle
194 ps decay time
PCD03Kapton16
PCD Signal (V)
Time (sec)
1
0.8
0.6
0.4
0.2
0
-0.2
0
1 10-9
2 10-9
3 10-9
4 10-9
5 10-9

Figure 2

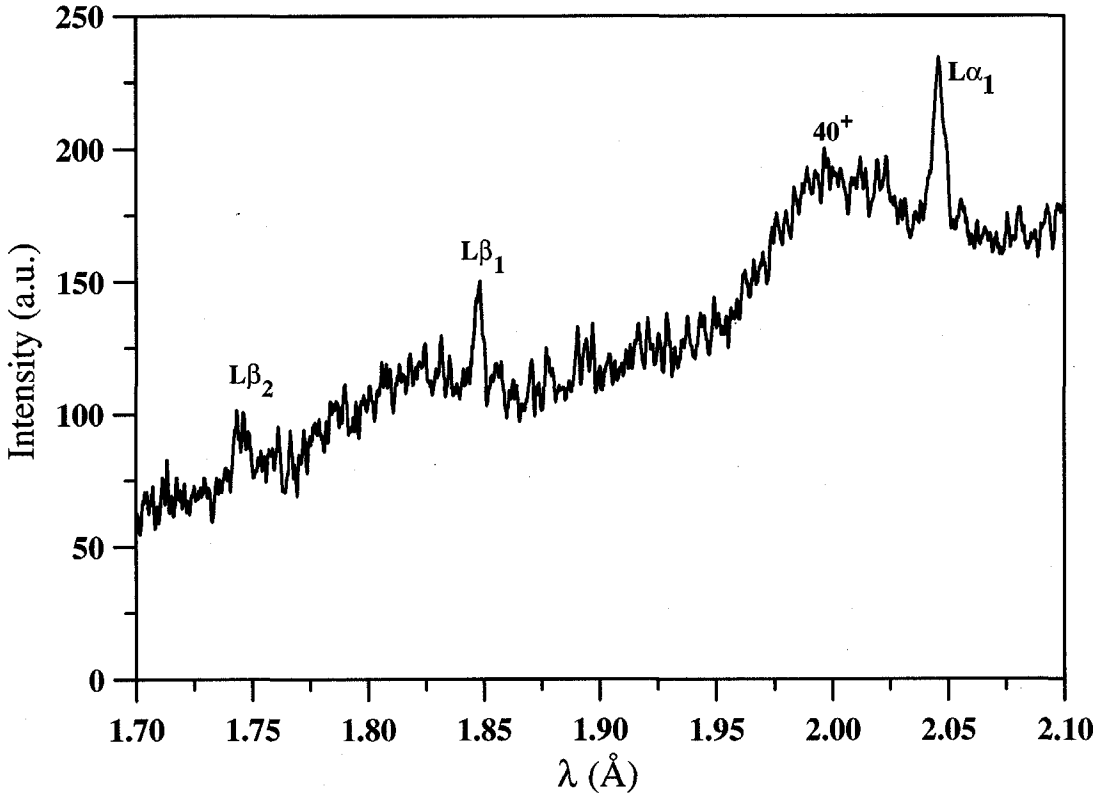
250
200
150
100
50
0
Intensity (a.u.)
1.70
1.75
1.80
1.85
1.90
1.95
2.00
2.05
2.10
λ (Å)
Lβ2
Lβ1
40+
Lα1

Figure 3a

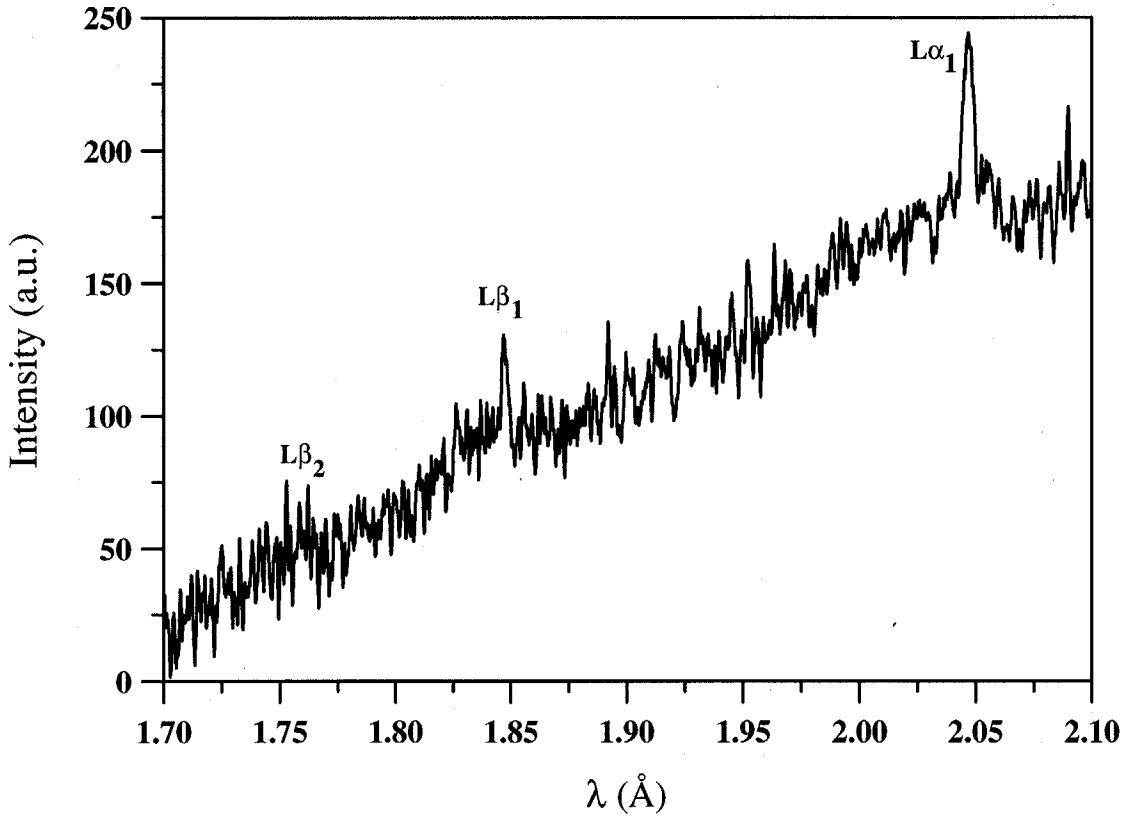
Intensity (a.u.)
250
200
150
100
50
0
1.70
1.75
1.80
1.85
1.90
1.95
2.00
2.05
2.10
λ (Å)
Lα1
Lβ1
Lβ2

Figure 3b

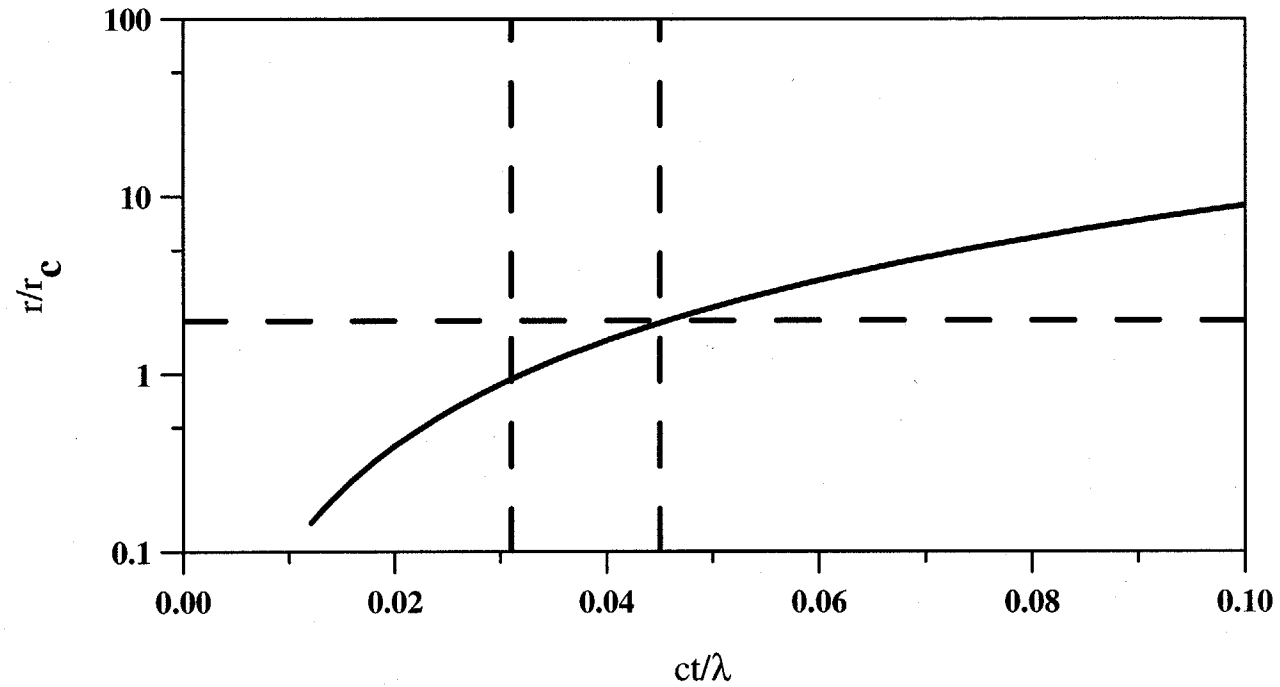

Figure 4a

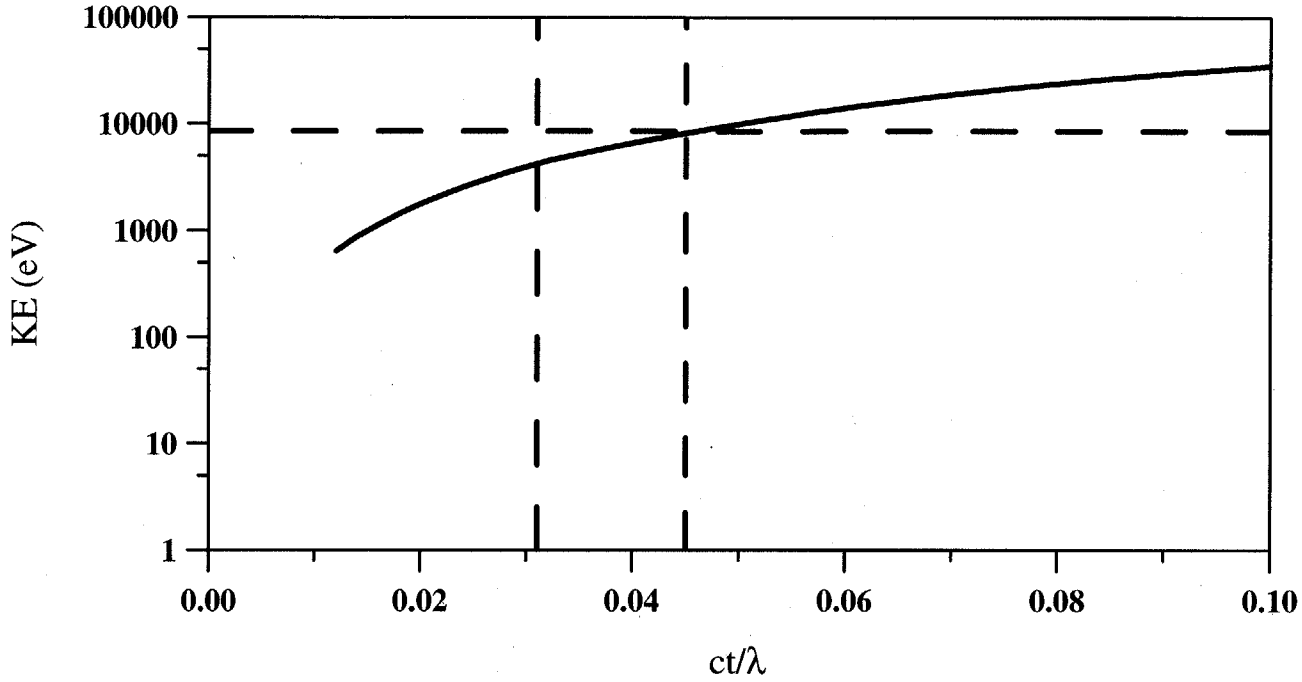

Figure 4b

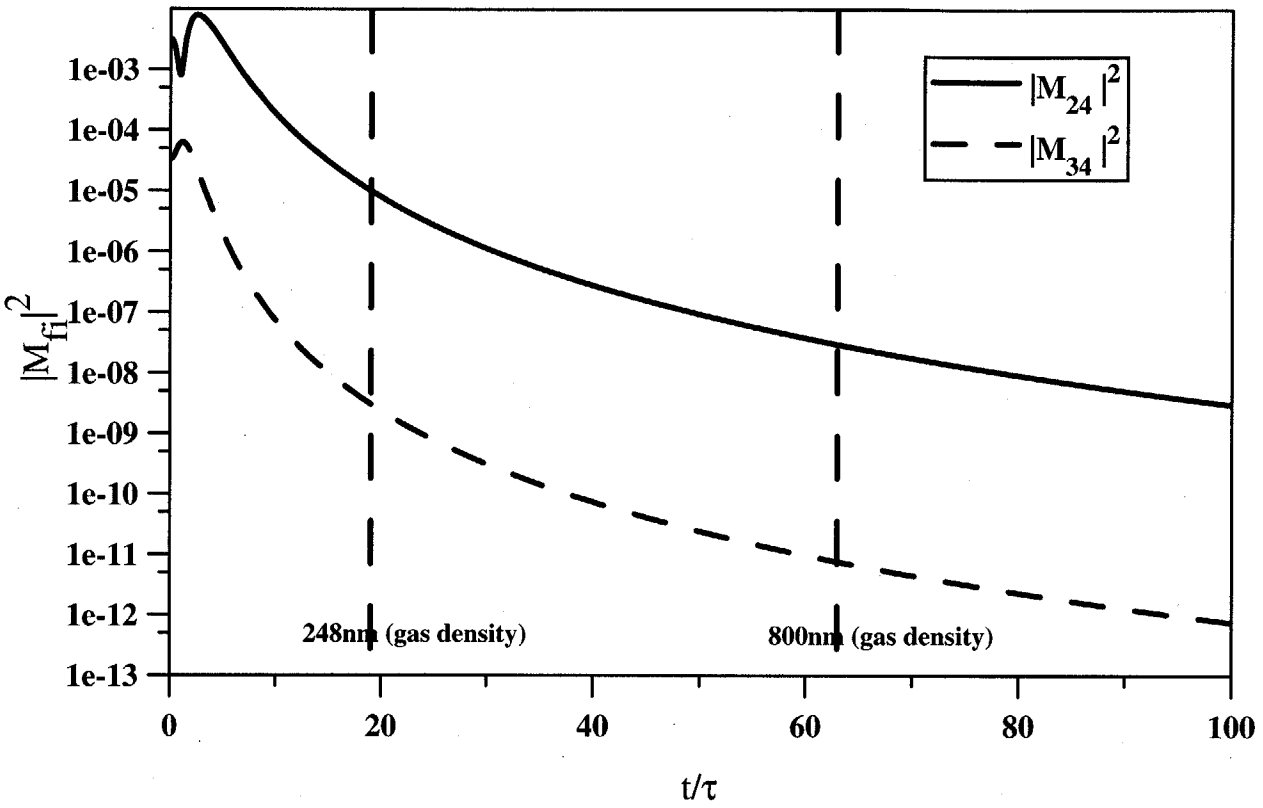
1e-03
1e-04
1e-05
1e-06
1e-07
1e-08
1e-09
1e-10
1e-11
1e-12
1e-13
$|M_{fi}|^2$
$|M_{24}|^2$
$|M_{34}|^2$
248nm (gas density)
800nm (gas density)
0
20
40
60
80
100
t/τ

Figure 5a

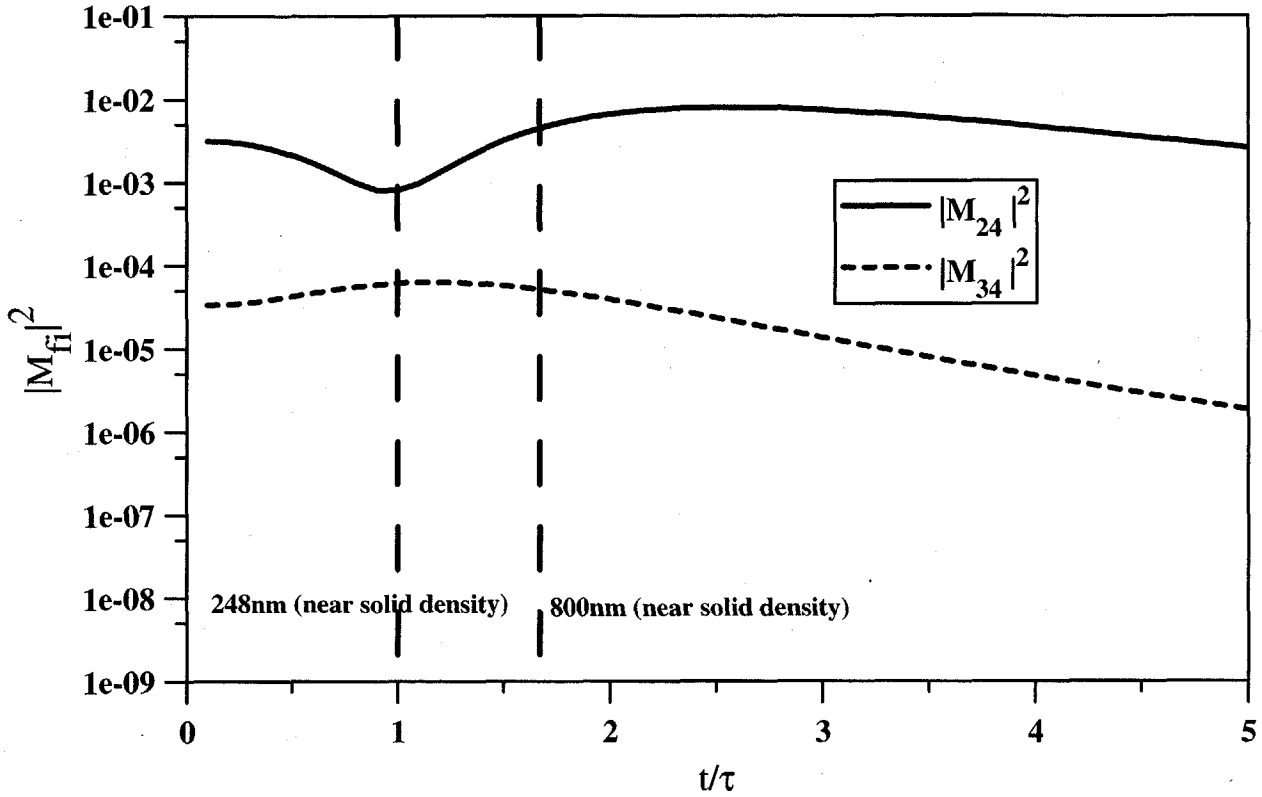
1e-01
1e-02
1e-03
1e-04
1e-05
1e-06
1e-07
1e-08
1e-09
$|M_{fi}|^2$
$|M_{24}|^2$
$|M_{34}|^2$
248nm (near solid density)
800nm (near solid density)
0
1
2
3
4
5
t/τ

Figure 5b

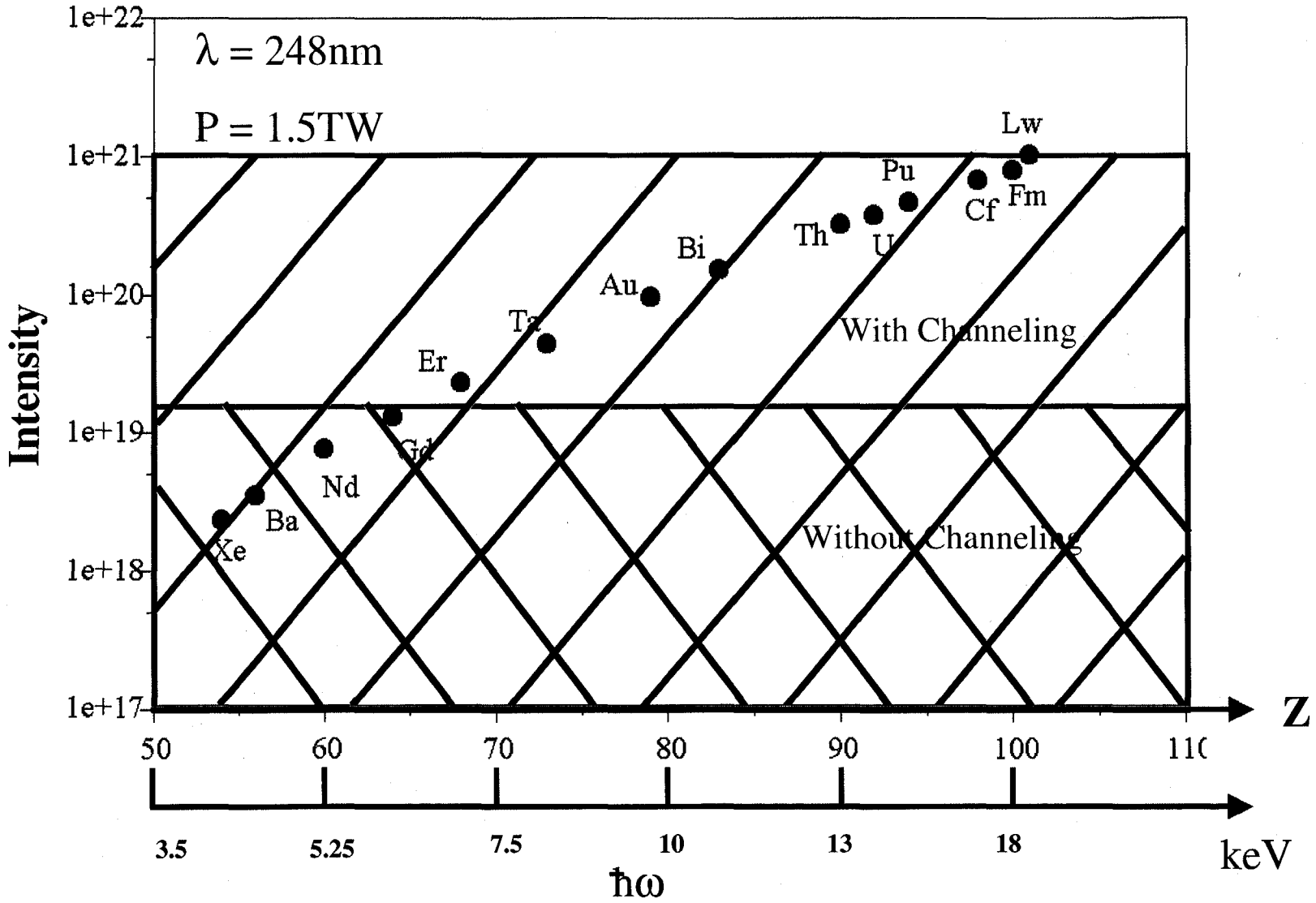
λ = 248nm
P = 1.5TW
Intensity
1e+22
1e+21
1e+20
1e+19
1e+18
1e+17
Lw
Pu
Cf
Fm
Th
U
Bi
Au
Ta
Er
Gd
Nd
Ba
Xe
With Channeling
Without Channeling
Z
50
60
70
80
90
100
110
3.5
5.25
7.5
10
13
18
keV
ħω

Figure 6

Material	Ionization Potential I_p (eV) For 4p electrons	Charge State	I_{ATI} (W cm^{-2})
Ba	~ 670 - 880	20^+ - 25^+	4 x 10^{18}
Gd	~ 1100 - 1400	28^+ - 33^+	1.4 x 10^{19}
Ta	~1700 - 2100	37^+ - 42^+	4.4 x 10^{19}
Au	~2300 - 2700	43^+ - 48^+	9 x 10^{19}
U	~3700 - 4350	56^+ - 61^+	3.7 x 10^{20}

Table I

Figure Captions

Figure 1.

Ba(L) Ionized plasma spectrum + characteristic lines from weakly ionized ($< \sim 10^{+}$), produced by intense irradiation (10^{19} W/cm^2) of a BaF_2 target. The peak has a charge state of 38^{+} as labeled on the plot.

Figure 2.

Diamond PCD signal of the L-shell radiation from BaF_2. The trace shows a rise time of ~150ps for the detector. The calibration of 160μA/W corresponds to an energy of ~4.9mJ of energy, assuming a 2π radiation distribution.

Figure 3

(a.) Gd(L) Ionized plasma spectrum + characteristic lines from weakly ionized ($< \sim 10^{+}$) Gd ions, produced by intense irradiation (10^{19} W/cm^2) of a 100μm thick Gd foil.

(b.) Gd(L) characteristic line spectrum only, produced by peak intensities a factor of 0.6 less than figure 3(a).

Figure 4.

(a.) Electron displacement vs. time. Results from the fully relativistic numerical simulation of the kinematic motion of an electron for an intensity of I = 10^{19}W/cm^2 under the influence of the electric and magnetic fields of 248nm (UV) radiation, data taken from Reference [7] by permission. Plot is in units of radius for a cluster of 13 Xe atoms ($r_c \approx 5.3$Å). The horizontal line indicates $r/r_c = 2$.

(b.) Electron Kinetic Energy vs. time. Horizontal line corresponds to 8500eV, the approximate ionization potential for a 2p electron in Ba. The vertical lines in both plots indicate the times at which an electron reaches $r/r_c = 1$, and 2.

Figure 5.

Plot of $|M_{fi}|^2$ for Ba.

(a.) The long dashed vertical lines correspond to 248nm ($t/\tau = 19$) and 800nm ($t/\tau = 63$), in the case of a gas cluster target, illustrating the values of $|M_{fi}|^2$ for the case of the upper limit on the ion spacing.

(b.) The long dashed lines correspond to the 248nm($t/\tau = 1$) and 800nm($t/\tau = 1.67$) for the case where the average ion spacing is twice the lattice spacing, illustrating the lower limit on the ion separation. As can be seen, the wavelength dependence would be much less severe in this limit.

Figure 6.

Map of required laser intensities to generate hollow atom L-shell spectrum for various elements, shown according to Z. The second horizontal axis shows the photon energy for L-shell radiation from the respective elements.

Table I.

Ionization potentials and required laser intensities to ionize the $4p$ electrons by above threshold ionization (ATI) in various solid elements.

References

1. McPherson A., Thompson B.D., Borisov A.B., Boyer K. and Rhodes C.K.: Multiphoton-induced x-ray emission at 4-5keV from Xe atoms with multiple core vacancies. Nature 370:631-634, 1994.
2. McPherson A., Luk T.S., Thompson B.D., Borisov A.B., Shiryaev O.B., Chen X., Boyer K. and Rhodes C.K.: Multiphoton-induced x-ray emission from Kr clusters on M-shell (~100Å) and L-shell (~6Å) transitions. Physical Review Letters 72:1810-1813, 1994.
3. McPherson A., Boyer K. and Rhodes C.K.: X-ray superradiance from multiphoton excited clusters. Journal of Physics B 27:L637-L641, 1994.
4. Ditmire T., Patel P.K., Smith R.A., Wark J.S., Rose S.J., Milathianaki D., Marjoribanks R.S. and Hutchinson M.H.R.: keV x-ray spectroscopy of plasmas produced by the intense picosecond irradiation of a gas of Xenon clusters. Journal of Physics B 31:2825-2831, 1998.
5. Ditmire T., Donnelly T., Falcone R.W. and Perry M.D.: Strong x-ray emission from the high temperature plasmas produced by intense irradiation of clusters. Physical Review Letters 75:3122-3125, 1995.
6. Kondo K., Borisov A.B., Jordan C., McPherson A., Schroeder W.A., Boyer K. and Rhodes C.K.: Wavelength dependence of multiphoton-induced Xe(M) and Xe(L) emissions from Xe clusters. Journal of Physics B 30:2707-2716, 1997.
7. Schroeder W.A., Omenetto F.G., Borisov A.B., Longworth J.W., McPherson A., Jordan C., Boyer K., Kondo K. and Rhodes C.K.: Pump laser wavelength-dependent control of the efficiency of kilovolt x-ray eimssion from atomic clusters. Journal of Physics B. 31:5031-5051, 1998.
8. Schroeder W.A., Nelson T.R., Borisov A.B., Longworth J.W., Boyer K. and Rhodes C.K.: An efficient, selective collisional ejection mechanism for inner-shell population inversion in laser-driven plasmas. Submitted Journal of Physics B.
9. Omenetto F.G., Boyer K., Longworth J.W., McPherson A., Nelson T.R., Schroeder W.A., Rhodes C.K., Marowsky G. and Szamtari S.: High brightness terawatt KrF* (248nm) system. Applied Physics B 64:643-646, 1997.
10. Nelson T.R., Schroeder W.A., Rhodes C.K., Omenetto F.G. and Longworth J.W.: Short pulse amplification at 745nm in Ti:Sapphire with a continuously tunable regenerative amplifier. Applied Optics 36: 7752-7755, 1997.
11. Cowan, R.D.: The Theory of Atomic Structure and Spectra. Berkeley, CA, University of California Press, 1981.
12. Tsuda N. and Yamada J.: Physical properties of dense plasma produced by XeCl excimer laser in high-pressure Argon gases. Jap. J. Applied Physics Part 1 38:3712-3715, 1999.
13. Ditmire T., Springate E., Tisch J.W.G., Shao Y.L., Mason M.B., Hay N., Marangos J.P. and Hutchinson M.H.R.: Explosion of atomic clusters heated by high intensity femtosecond laser pulses. Physical Review A. 57:369-382, 1998.
14. Protopapas M., Keitel C.H. and Knight P.L.: Atomic physics with super-high intensity lasers. Rep. Prog. Phys. 60:389,1997.

15. Ammosov M.V., Delone N.B. and Krainov V.P.: Tunnel ionization of complex atoms and atomic ions in electromagnetic field. Sov. Phys.- JETP 64:1191, 1986.
16. Carlson T.A., Nestor C.W. Jr., Wasserman N. and McDowell J.D.: Calculated ionization potentials for multiply charged ions. Atomic Data 2:63-99, 1970.
17. Borisov A.B., Longworth J.W., Boyer K. and Rhodes C.K.: Stable relativistic/charge displacement channels in ultrahigh power density ($\sim 10^{21}$W/cm^3) plasmas. Proc. Natl. Acad. Sci. USA 95:7854-7859, 1998.
18. Borisov A.B., McPherson A., Thompson B.D., Boyer K. and Rhodes C.K.: Ultra-high power compression for x-ray amplification – multiphoton cluster excitation combined with nonlinear channeled propagation. Journal of Physics B. 28:2143–2158, 1995.
19. Gahn C., Pretzler G., Saemann A., Tsakiris G.D., Witte K.J., Gassmann D., Schätz T., Schramm U., Thirolf P. and Habs D.: MeV gamma-ray yield from solid targets irradiated with fs-laser pulses. Applied Physics Letters 73:3662-3664, 1998.
20. Ditmire T., Donnelly T., Rubenchik A.M., Falcone R.W., and Perry M.D.: Interaction of intense laser pulses with atomic clusters. Physical Review A 55:3379 – 3402, 1996.
21. McGuire E.J.: Scaled electron ionization cross sections in the Born approximation. Physical Review A. 16:73 – 79, 1977.